DISORDERED BINDING OF SMALL MOLECULES TO A$\beta_{12\text{-}28}$

Marino Convertino, Andreas Vitalis*, and Amedeo Caflisch*

Department of Biochemistry, University of Zurich, Winterthurerstrasse 190, CH-8057 Zurich, Switzerland

Supplemental Data

Address correspondence to:

Prof. Dr. Amedeo Caflisch, Winterthurerstrasse 190, CH-8057 Zurich, Switzerland.
Tel: +41 44 635 55 21; fax: +41 44 635 68 62; E-mail: caflisch@bioc.uzh.ch.

Dr. Andreas Vitalis, Winterthurerstrasse 190, CH-8057 Zurich, Switzerland.
Tel: +41 44 635 55 97; fax: +41 44 635 68 62; E-mail: a.vitalis@bioc.uzh.ch.

Table S1. Percentage of molecular dynamics snapshots similar to the representative loop conformation obtained in the presence of NQTrp using 1.5 Å and 2.0 Å cutoffs in RMSD computed over the Cα atoms of residues 14-24.

Inhibitor [a]	**3 blocks** [b]				**6 blocks** [b]			
(cutoff 1.5 Å)	**μ**	**σ**	**MAX**	**min**	**μ**	**σ**	**MAX**	**min**
A$\beta_{12\text{-}28}$	1.8	1.1	2.9	1.0	1.8	1.4	4.2	0.2
NQTrp	19.0	15.3	40.1	4.4	19	17.6	48.7	0.4
9,10-anthraquinone	8.2	6.3	15.5	0.2	8.2	10.8	30.4	0.2
anthracene	5.4	3.6	9.7	0.9	5.4	4.8	11.4	0.3
Tyr-Aib-Trp-Phe	4.5	1.6	6.3	2.4	4.5	4.9	12.5	0.1
Tyr-Pro-Trp-Phe	5.1	2.7	8.9	2.5	5.1	6.3	17.7	0.1
Tyr-Pro-Phe-Phe	5.2	2.4	8.3	2.4	5.2	4.8	14.6	0.2
Tyr-Pro-Trp-Phe-NH_2	7.4	3.8	10.9	3.4	7.4	5.8	15.3	0.4
Tyr-Pro-Phe-Phe-NH_2	4.3	2.8	7.4	2.1	4.3	3.3	8.0	0.2
^{D}Trp-Aib	6.9	6.5	16.1	1.7	6.9	11.2	31.7	0.2
β-Ala-His	1.4	1.4	3.3	0.1	1.4	1.4	3.8	0.1
Inhibitor [a]	**3 blocks** [b]				**6 blocks** [b]			
(cutoff 2.0 Å)	**μ**	**σ**	**MAX**	**min**	**μ**	**σ**	**MAX**	**min**
A$\beta_{12\text{-}28}$	2.9	1.3	4.3	1.6	2.9	1.7	5.5	0.9
NQTrp	22.5	14.0	41.6	8.5	22.5	16.3	50.0	5.4
9,10-anthraquinone	10.3	7.1	18.3	1.1	10.3	11.4	33.3	0.7
anthracene	6.8	3.7	11.1	1.8	6.8	4.4	12.7	2.2
Tyr-Aib-Trp-Phe	6.1	1.5	8.2	4.6	6.1	4.4	14	1.5
Tyr-Pro-Trp-Phe	7.6	3.3	12.2	4.9	7.6	5.4	19.1	3.2
Tyr-Pro-Phe-Phe	16.6	1.1	18.2	15.4	16.6	2.0	20.6	14.3
Tyr-Pro-Trp-Phe-NH_2	11.7	2.2	14.1	9.8	11.7	5.7	18.0	1.6
Tyr-Pro-Phe-Phe-NH_2	9.9	5.9	16.5	5.1	9.9	8.0	25.3	1.6
^{D}Trp-Aib	8.3	6.9	18.0	2.4	8.3	11.4	33.3	0.7
β-Ala-His	2.2	1.6	4.4	0.6	2.2	1.7	5.5	0.4

[a]Aib: α-aminoisobutyric acid; NQTrp: 1,4-napthoquinon-2-yl-L-tryptophan; β-Ala-His: carnosine.

[b]Block averaging was performed by dividing the 15 μs of total sampling into three 5 μs blocks (left) and six 2.5 μs blocks (right). μ and σ denote arithmetic mean and standard deviation, respectively, while MAX and min are the respective maximum and minimum values for each set of blocks.

Table S2. Decomposition of effective binding energy into individual terms. All values are given in kcal/mol.

Inhibitor [a]	sampling [g]	vdW [b]	ELEC [c]	FCTPL [d]	FCTNP [e]	TOTAL [f]
NQTrp	*full*	-15.8	-12.9	17.7	-3.0	-13.9
	1st block	-15.1	-13.4	18.1	-2.9	-13.4
	2nd block	-18.4	-15.2	20.3	-3.3	-16.6
	3rd block	-13.7	-9.9	14.6	-2.8	-11.8
9,10-anthraquinone	*full*	-6.6	-2.9	5.4	-1.5	-5.6
	1st block	-8.1	-5.4	8.1	-1.7	-6.9
	2nd block	-6.9	-3.1	5.7	-1.5	-5.9
	3rd block	-4.9	-0.3	2.6	-1.4	-4.1
anthracene	*full*	-7.7	0.1	1.8	-1.7	-7.5
	1st block	-8.1	-1.3	3.2	-1.8	-7.9
	2nd block	-6.1	2.35	-0.6	-1.6	-5.9
	3rd block	-8.8	-0.77	2.9	-1.9	-4.1
Tyr-Aib-Trp-Phe	*full*	-9.6	-8.8	12.1	-2.8	-9.2
	1st block	-9.5	-9.5	12.6	-2.8	-9.2
	2nd block	-8.8	-6.9	10.2	-2.7	-8.3
	3rd block	-10.5	-10.1	13.4	-2.9	-10.1
Tyr-Pro-Trp-Phe	*full*	-10.3	-10.7	14.1	-2.9	-9.8
	1st block	-11.5	-13.3	16.8	-3.1	-11
	2nd block	-9.9	-7.8	10.9	-2.8	-8.5
	3rd block	-10.3	-11.2	14.5	-2.9	-9.9
Tyr-Pro-Phe-Phe	*full*	-16.3	-14.7	19.1	-3.6	-15.6
	1st block	-16.9	-16.4	20.6	-3.6	-16.3
	2nd block	-16.8	-14.7	19.1	-3.7	-15.9
	3rd block	-15.3	-13.1	17.4	-3.5	-14.5
Tyr-Pro-Trp-Phe-NH_2	*full*	-11.9	-5.9	10.0	-3.3	-11.1
	1st block	-11.9	-7.0	11.1	-3.3	-11.2
	2nd block	-10.6	-4.3	8.2	-3.1	-9.9
	3rd block	-13.0	-6.4	10.8	-3.4	-12.0

Tyr-Pro-Phe-Phe-NH_2	*full*	-10.5	-7.0	10.5	-3.0	-10.0
	1st block	-12.7	-10.1	13.9	-3.3	-12.1
	2nd block	-7.2	-2.9	5.8	-2.6	-7.0
	3rd block	-11.2	-7.5	11.2	-3.1	-10.6
^{D}Trp-Aib	*full*	-4.5	-5.5	7.3	-1.8	-4.5
	1st block	-3.1	-5.5	6.8	-1.6	-3.3
	2nd block	-3.7	-2.9	4.6	-1.7	-3.6
	3rd block	-6.8	-8.1	10.3	-2.0	-6.6
β-Ala-His	*full*	-0.9	-4.9	5.7	-0.8	-0.8
	1st block	-0.5	-4.6	5.3	-0.8	-0.7
	2nd block	-0.5	-4.7	5.7	-0.7	-0.3
	3rd block	-1.7	-5.2	6.2	-0.9	-1.5

[a]Aib: α-aminoisobutyric acid; NQTrp:1,4-napthoquinon-2-yl-L-tryptophan; β-Ala-His: carnosine.

[b]vdW = van der Waals energy change upon binding

[c]ELEC = low-dielectric Coulombic energy upon binding

[d]FCTPL = change of electrostatic polarization upon binding calculated by FACTS (Haberthür and Caflisch, *J Comput Chem*, 2008)

[e]FCTNP = change of non-polar solvation energy calculated by FACTS using a surface tension-like parameter γ= 0.0075 kcal mol^{-1} $Å^{-2}$

[f]TOTAL = the total binding energy is the sum of the four preceding terms

[g]Block averaging was performed by dividing the 15 μs sampling into three 5 μs blocks. For further details, refer to Table 1 in the main text.

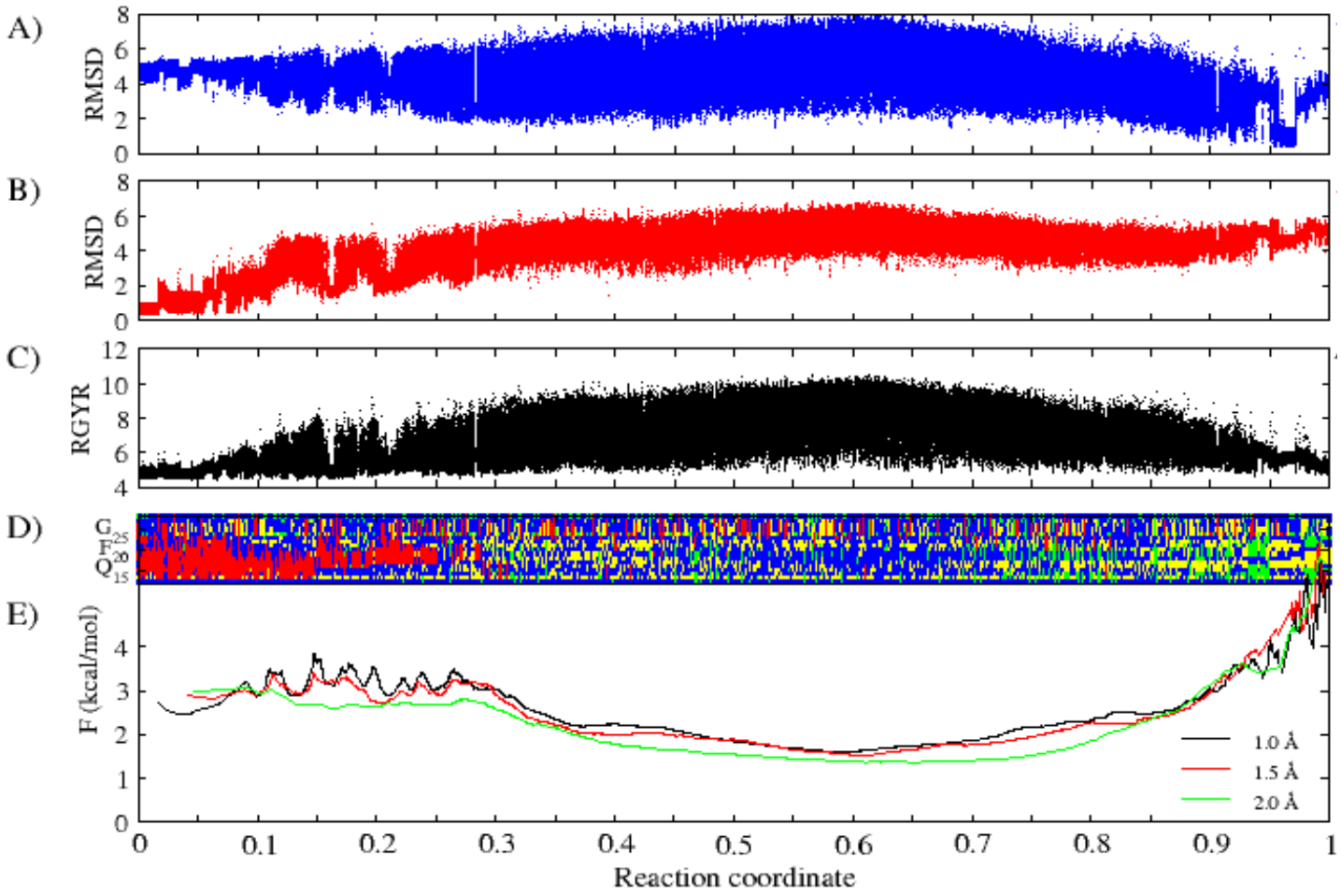

Figure S1. cFEP and other analyses of monomeric A$\beta_{12\text{-}28}$. The analysis in **A-D)** uses the snapshots rearranged according to the reaction coordinate in **E)**. **A)** Root mean square deviation (RMSD) of monomeric A$\beta_{12\text{-}28}$ from the cluster representative of the most populated node of A$\beta_{12\text{-}28}$ in presence of NQTrp. **B)** RMSD of monomeric A$\beta_{12\text{-}28}$ from its most populated conformer. **C)** Radius of gyration (RGYR) of monomeric A$\beta_{12\text{-}28}$. Cα atoms of residues 14-24 were used in RMSD and RGYR analyses. **D)** DSSP analysis of monomeric A$\beta_{12\text{-}28}$ (the color code is: helix in red; β-extended in green; loop and turn in blue; bend is plotted in yellow for clarity). The secondary structure analysis was calculated using the DSSPcont algorithm as implemented in Wordom (Seeber *et al*., *J Comput Chem* **32**, 1183 (2011)). **E)** cFEP plots starting from the most populated node of the conformational network as reference. Nodes are sorted according to their mean first passage time (mfpt) from the reference structure (for further details see Krivov and Karplus, *J \Phys Chem B*, **110**, 12689 (2006)). RMSD clustering over the Cα atoms of residues 14-24 of monomeric A$\beta_{12\text{-}28}$ with 1.0 Å (black), 1.5 Å (red), and 2.0 Å (green) cutoffs was used for cFEP analysis.

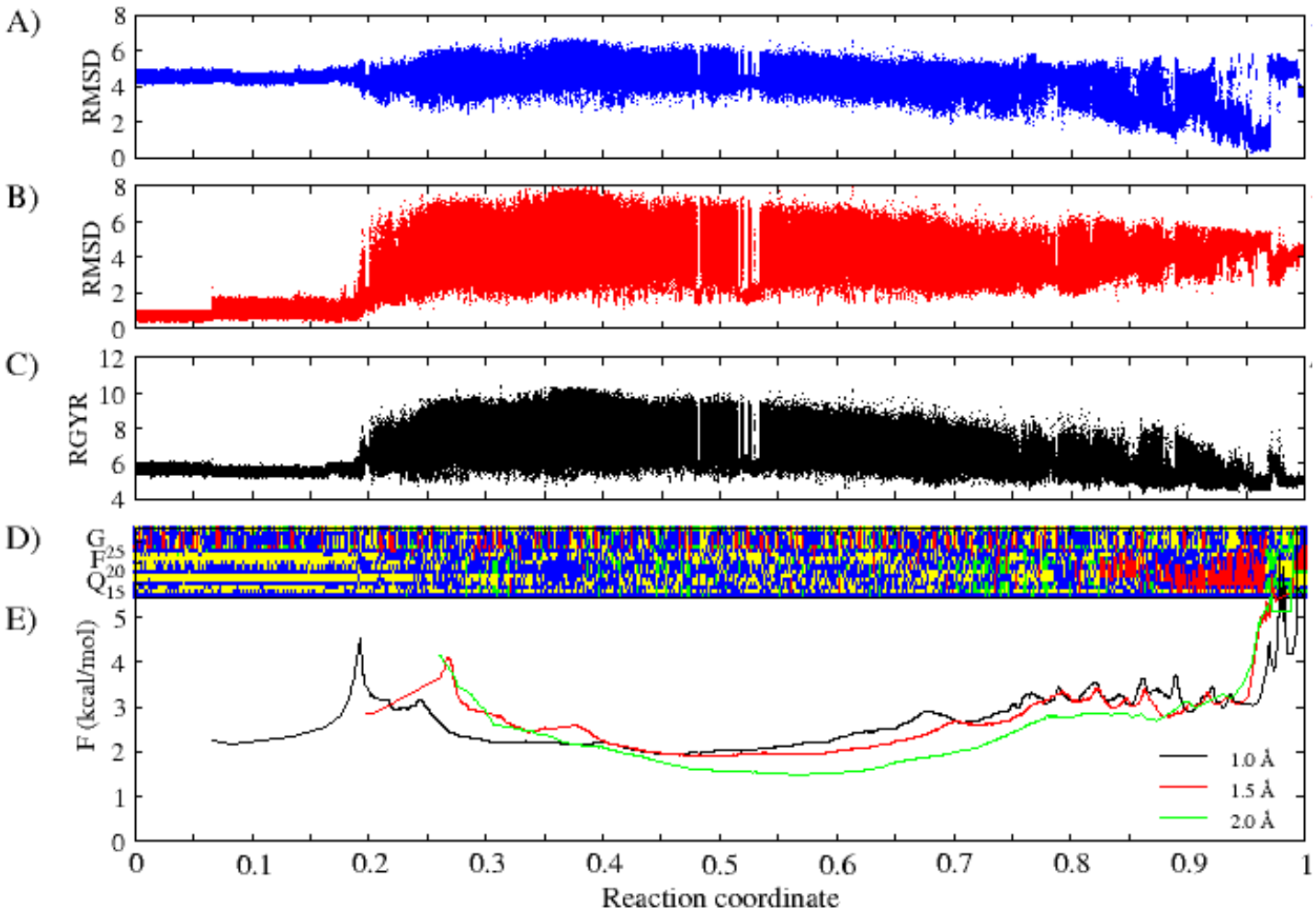

Figure S2. cFEP and other analyses of monomeric A$\beta_{12\text{-}28}$ in presence of NQTrp. The analysis in **A-D)** uses the snapshots rearranged according to the reaction coordinate in **E)**. **A)** RMSD of A$\beta_{12\text{-}28}$ in presence of NQTrp from the cluster representative of the most populated node of monomeric A$\beta_{12\text{-}28}$ alone. **B)** RMSD of A$\beta_{12\text{-}28}$ in presence of NQTrp from its most populated conformer. **C)** Radius of gyration (RGYR) of A$\beta_{12\text{-}28}$ in presence of NQTrp. Cα atoms of residues 14-24 were used in RMSD and RGYR analyses. **D)** DSSP analysis of monomeric A$\beta_{12\text{-}28}$ in presence of NQTrp (the color code is: helix in red; β-extended in green; loop and turn in blue; bend is plotted in yellow for clarity). **E)** cFEP plots starting from the most populated node of the conformational network as reference. Nodes are sorted according to their mean first passage time (mfpt) from the reference structure. RMSD clustering over the Cα atoms of residues 14-24 of monomeric A$\beta_{12\text{-}28}$ in presence of NQTrp with 1.0 Å (black), 1.5 Å (red), and 2.0 Å (green) cutoffs was used for cFEP analysis.

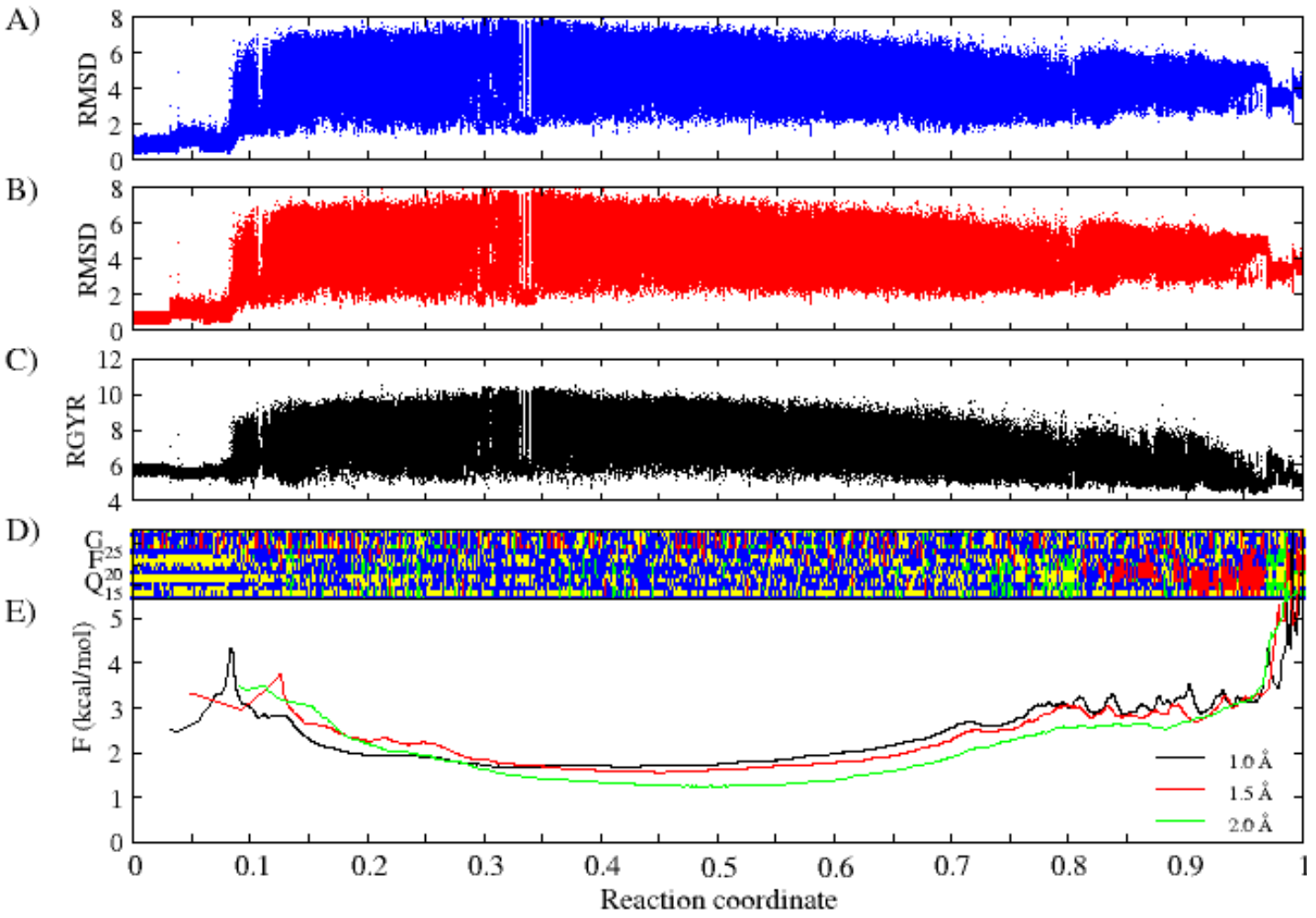

Figure S3. cFEP and other analyses of monomeric A$\beta_{12\text{-}28}$ in presence of 9,10-anthraquinone. The analysis in **A-D)** uses the snapshots rearranged according to the reaction coordinate in **E)**. **A)** RMSD of A$\beta_{12\text{-}28}$ in presence of 9,10-anthraquinone from the cluster representative of the most populated node of monomeric A$\beta_{12\text{-}28}$ in presence of NQTrp. **B)** RMSD of A$\beta_{12\text{-}28}$ in presence of 9,10-anthraquinone from its most populated conformer. **C)** Radius of gyration (RGYR) of A$\beta_{12\text{-}28}$ in presence of 9,10-anthraquinone. Cα atoms of residues 14-24 were used in RMSD and RGYR analyses. **D)** DSSP analysis of monomeric A$\beta_{12\text{-}28}$ in presence of 9,10-anthraquinone (the color code is: helix in red; β-extended in green; loop and turn in blue; bend is plotted in yellow for clarity). **E)** cFEP plots starting from the most populated node of the conformational network as reference. Nodes are sorted according to their mean first passage time (mfpt) from the reference structure. RMSD clustering over the Cα atoms of residues 14-24 of monomeric A$\beta_{12\text{-}28}$ in presence of 9,10-anthraquinone with 1.0 Å (black), 1.5 Å (red), and 2.0 Å (green) cutoffs was used for cFEP analysis.

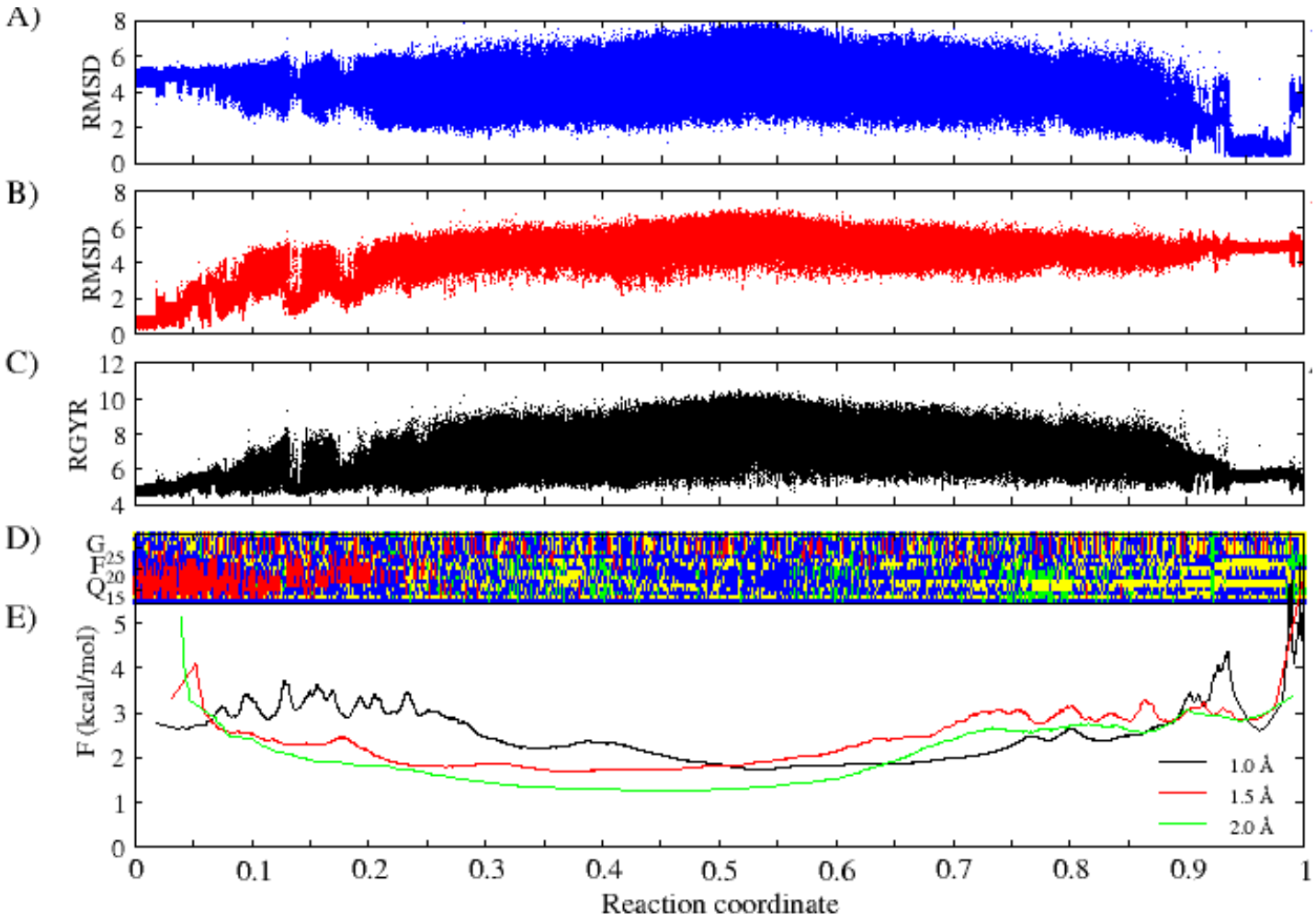

Figure S4. cFEP and other analyses of monomeric A$\beta_{12\text{-}28}$ in presence of anthracene.

Same as Figure S3 for anthracene.

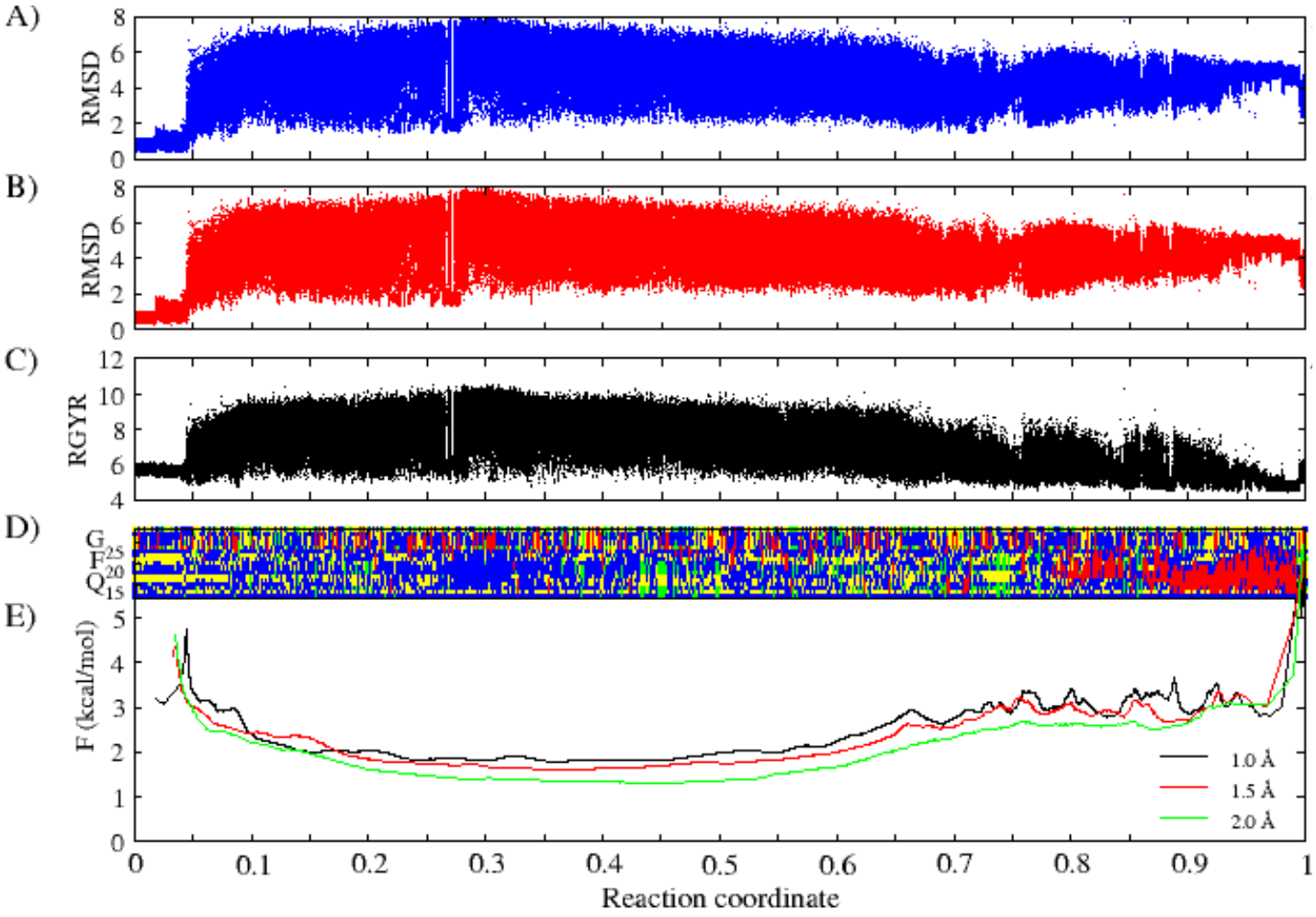

Figura S5. cFEP and other analyses of monomeric Aβ_{12-28} in presence of Tyr-Aib-Trp-Phe.

Same as Figure S3 for Tyr-Aib-Trp-Phe.

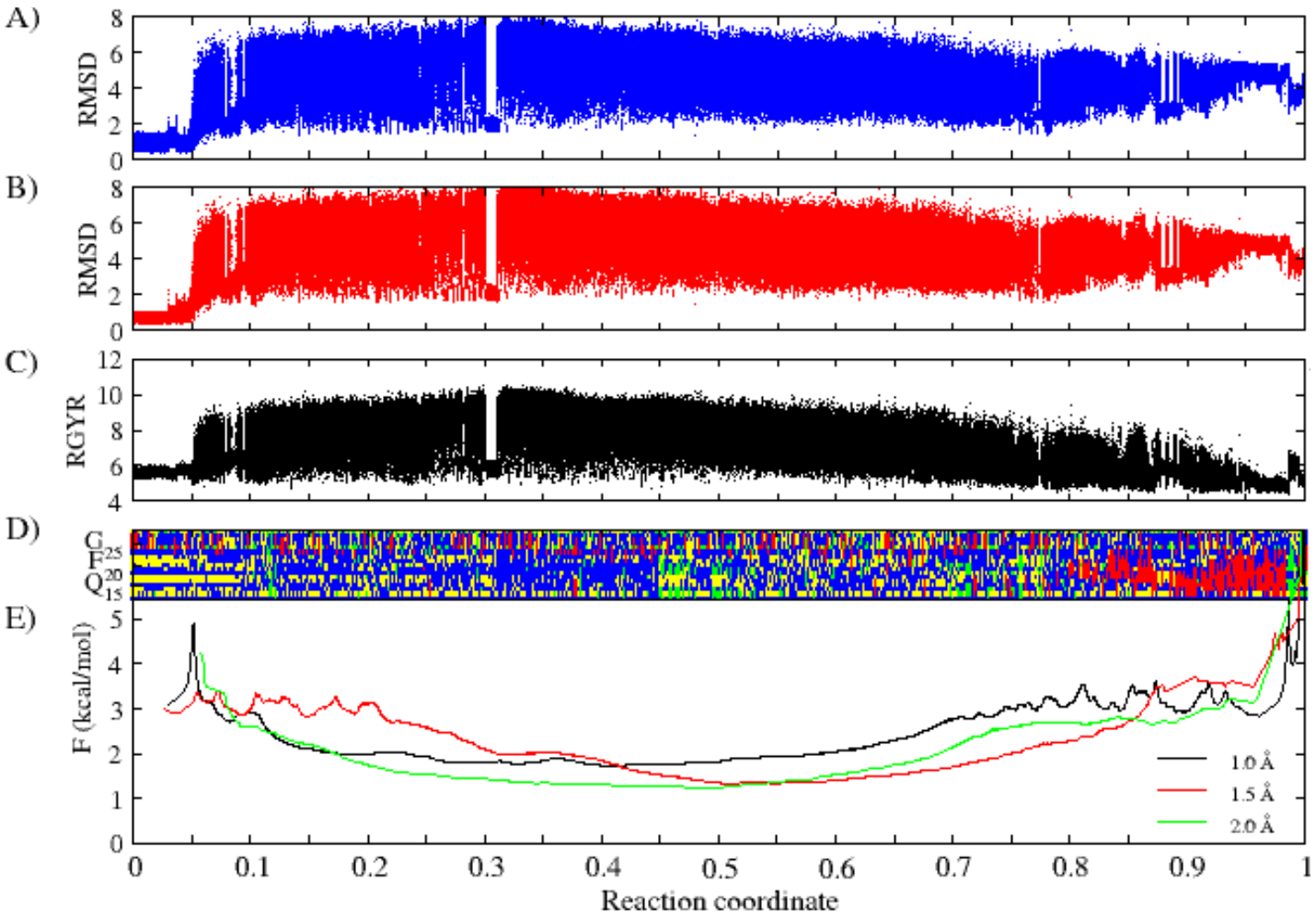

Figure S6. cFEP and other analyses of monomeric A$\beta_{12\text{-}28}$ in presence of Try-Pro-Trp-Phe.

Same as Figure S3 for Tyr-Pro-Trp-Phe.

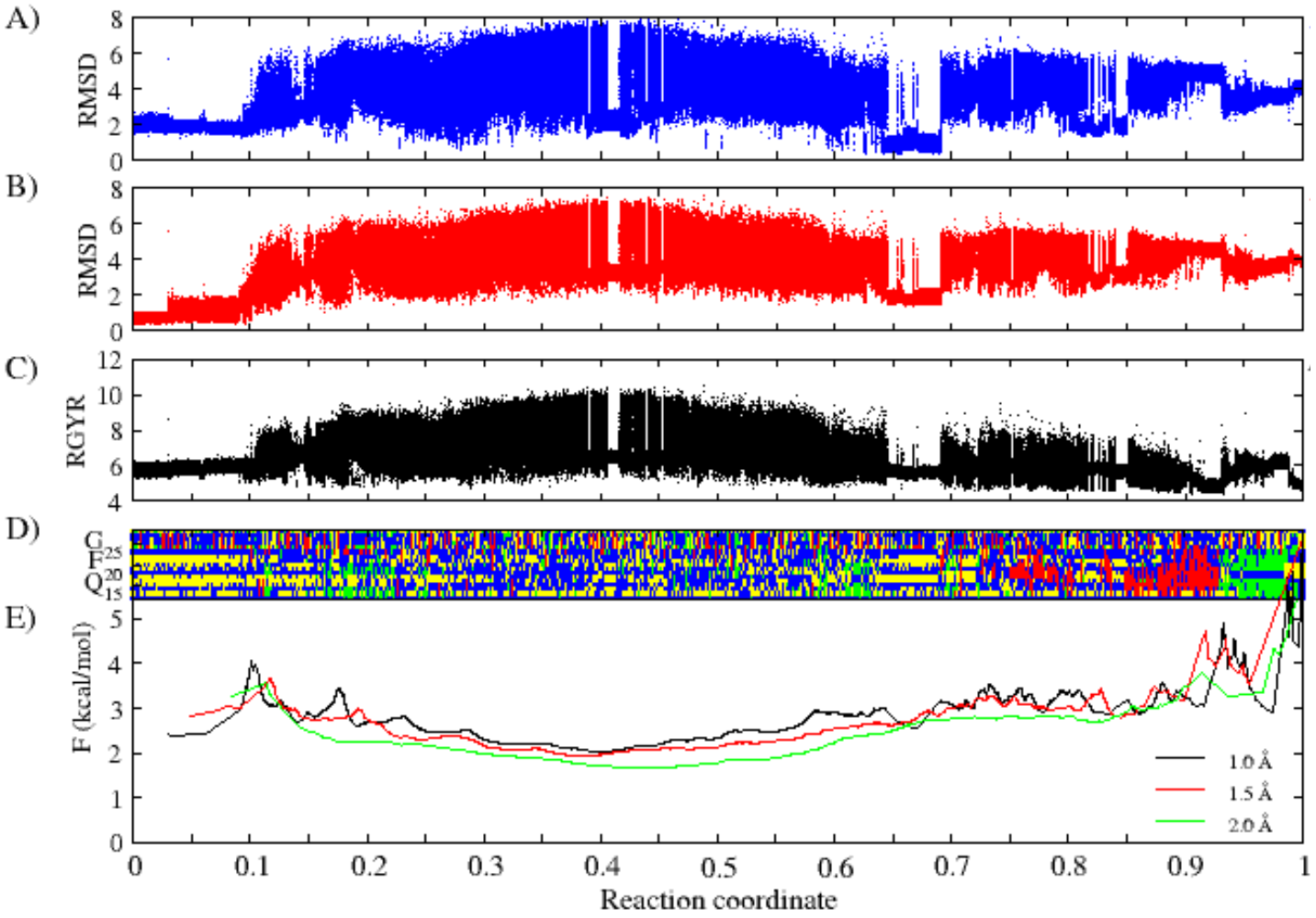

Figure S7. cFEP and other analyses of monomeric Aβ_{12-28} in presence of Tyr-Pro-Phe-Phe.

Same as Figure S3 for Tyr-Pro-Phe-Phe.

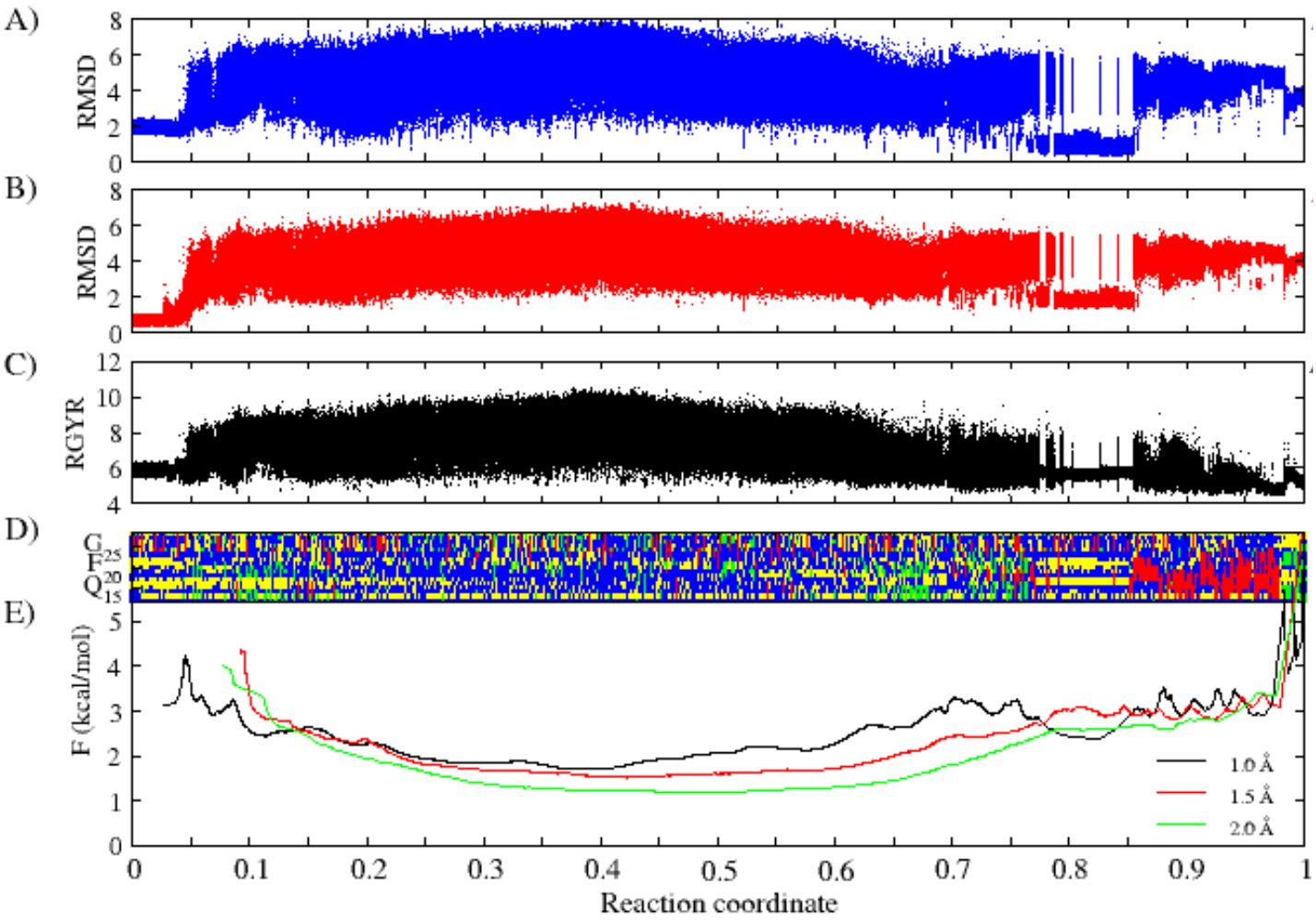

Figure S8. cFEP and other analyses of monomeric A$\beta_{12\text{-}28}$ in presence of Tyr-Pro-Trp-Phe-NH_2.

Same as Figure S3 for Tyr-Pro-Trp-Phe-NH_2.

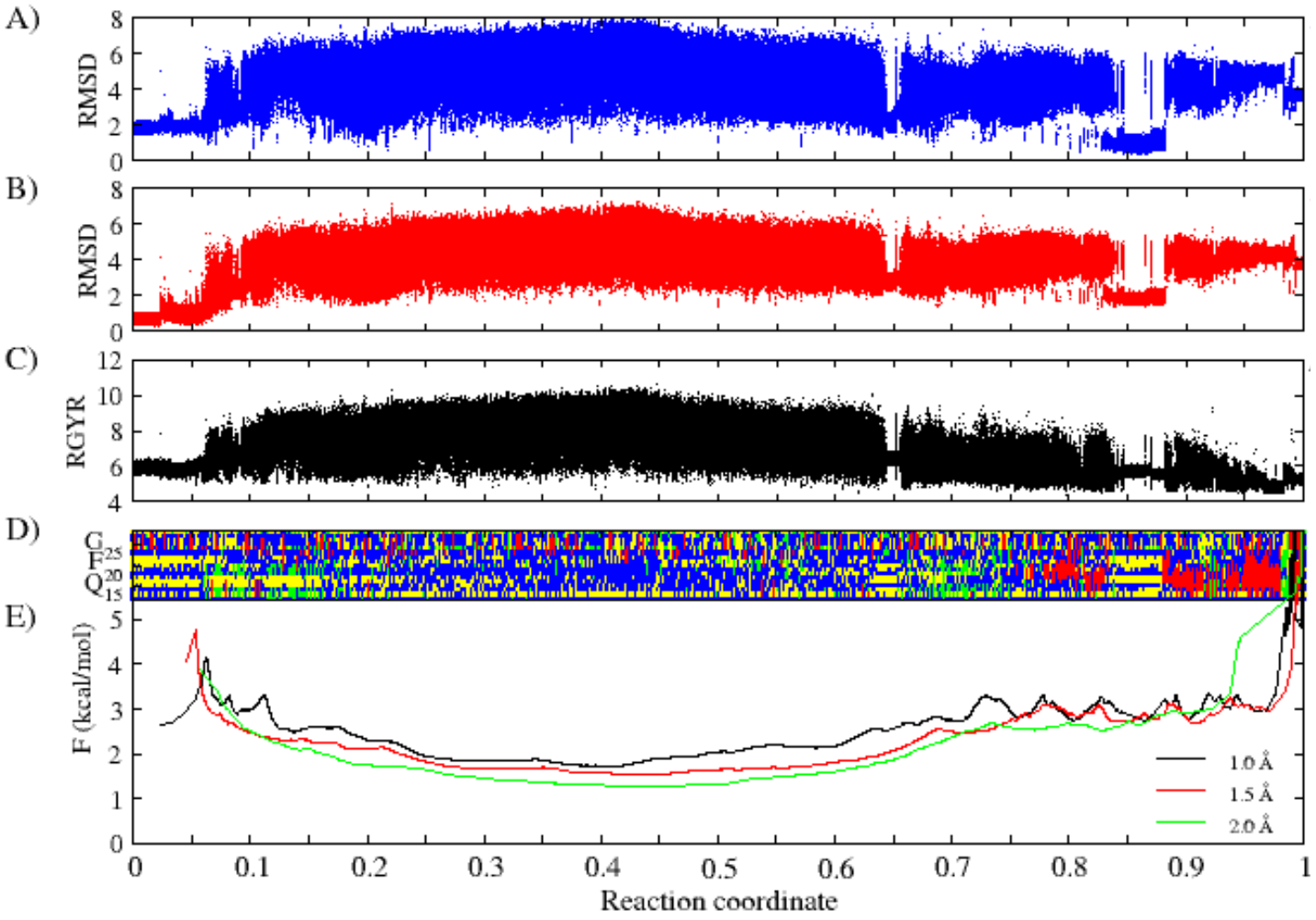

Figure S9. cFEP and other analyses of monomeric Aβ_{12-28} in presence of Tyr-Pro-Phe-Phe-NH_2.

Same as Figure S3 for Tyr-Pro-Phe-Phe-NH_2.

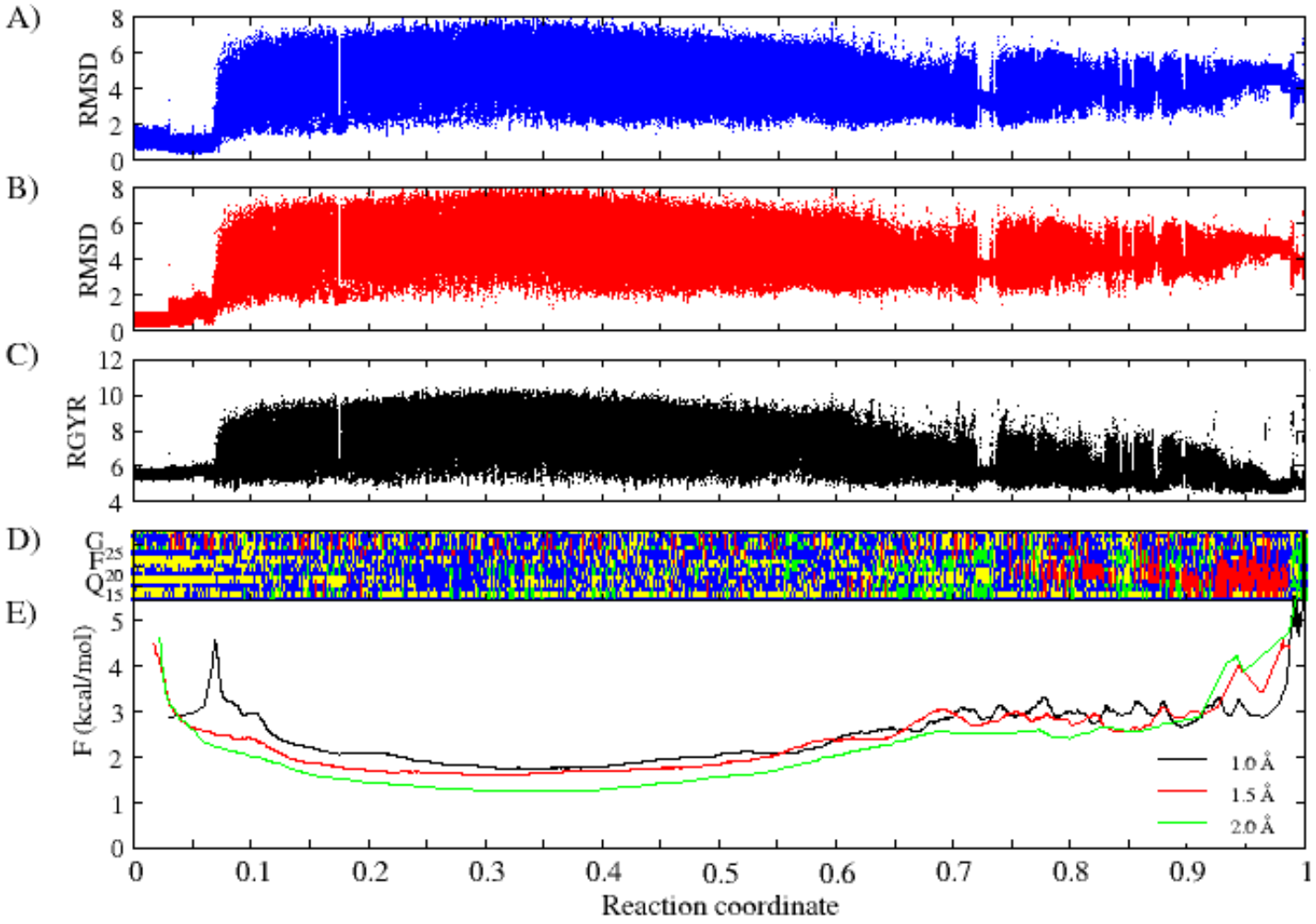

Figure S10. cFEP and other analyses of monomeric A$\beta_{12\text{-}28}$ in presence of ^{D}Trp-Aib.

Same as Figure S3 for ^{D}Trp-Aib.

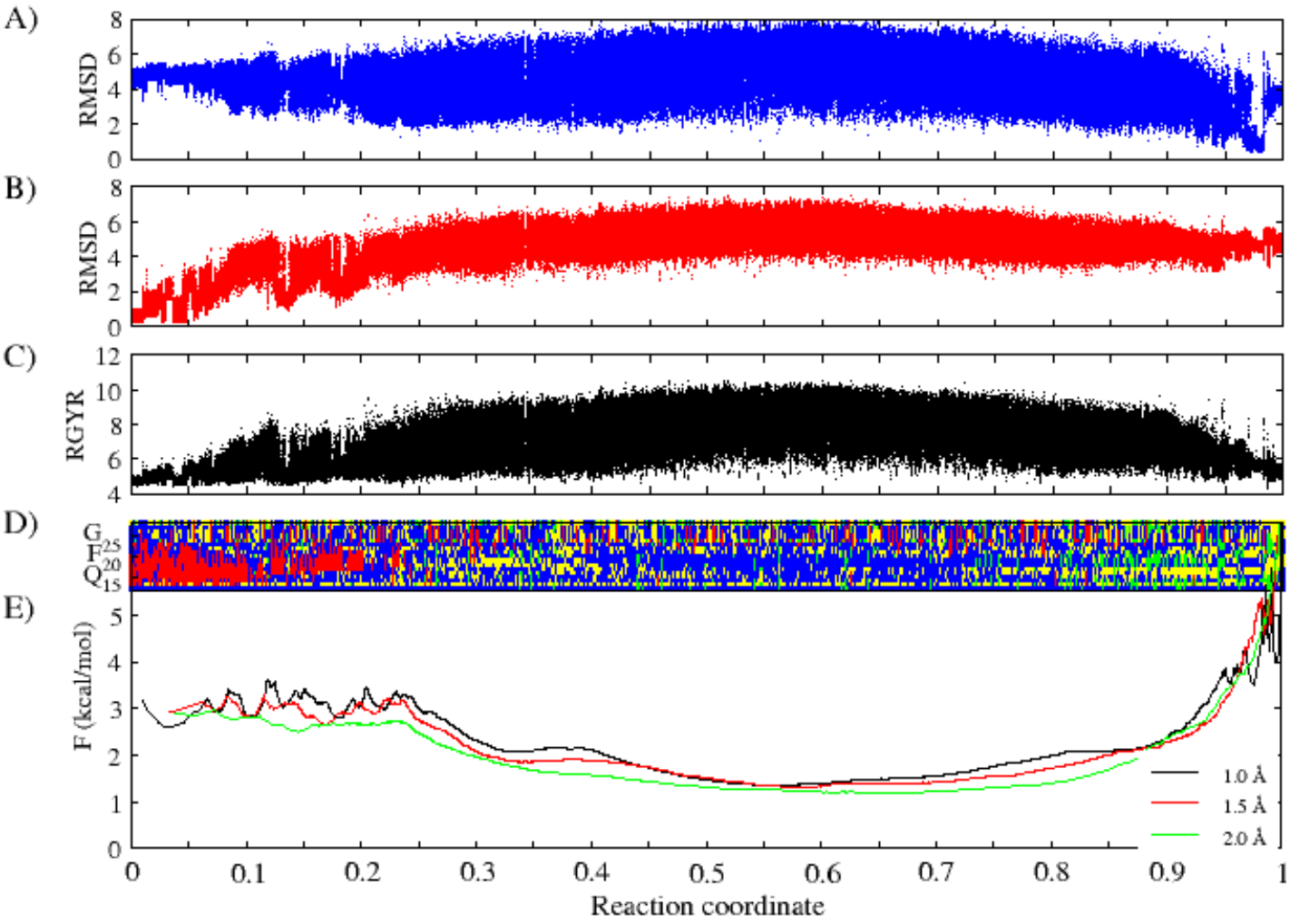

Figure S11. cFEP and other analyses of monomeric Aβ_{12-28} in presence of β-Ala-His.

Same as Figure S3 for β-Ala-His.

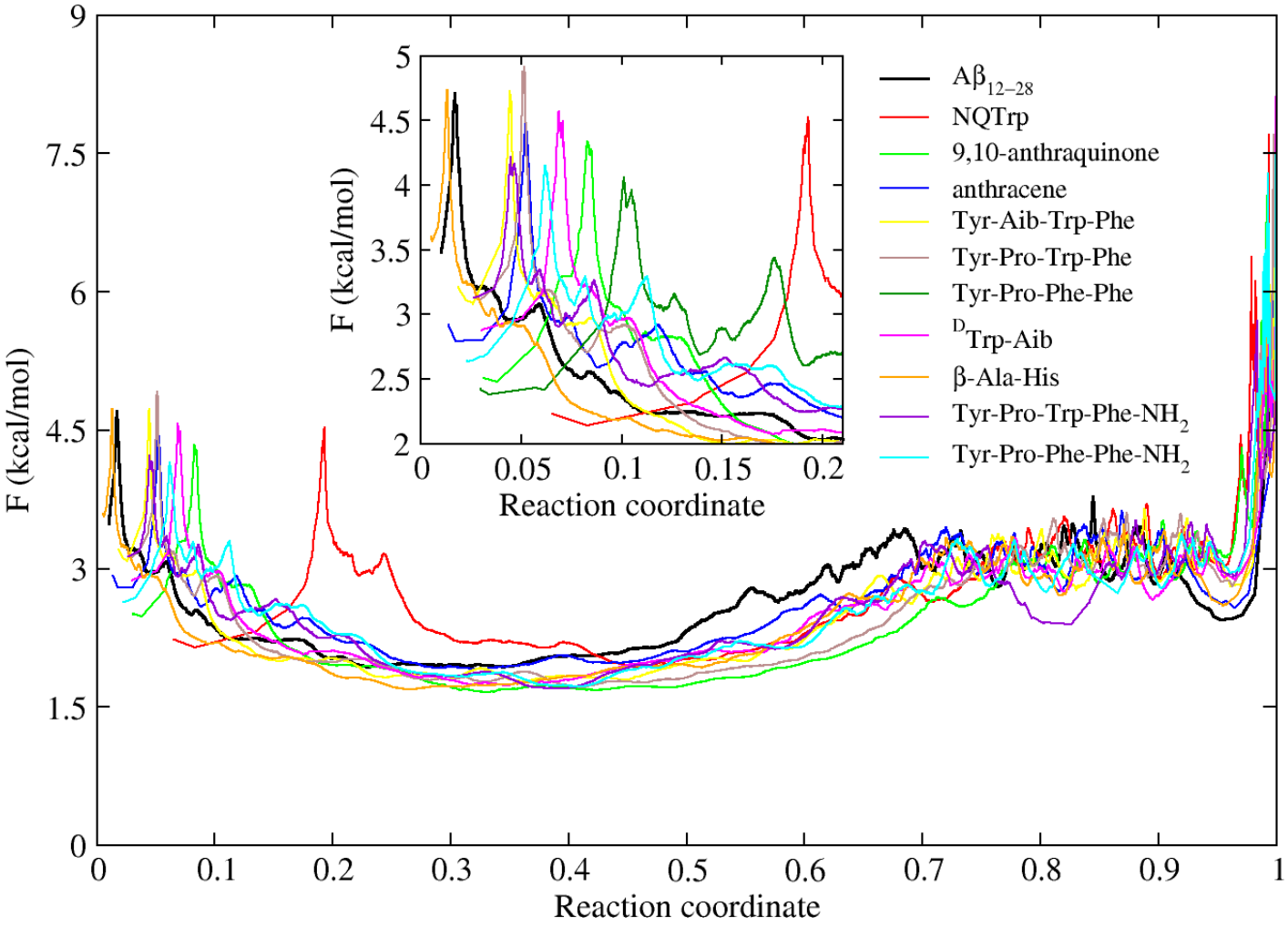

Figure S12. cFEP plots with the loop conformer as encountered in each simulation as reference state.

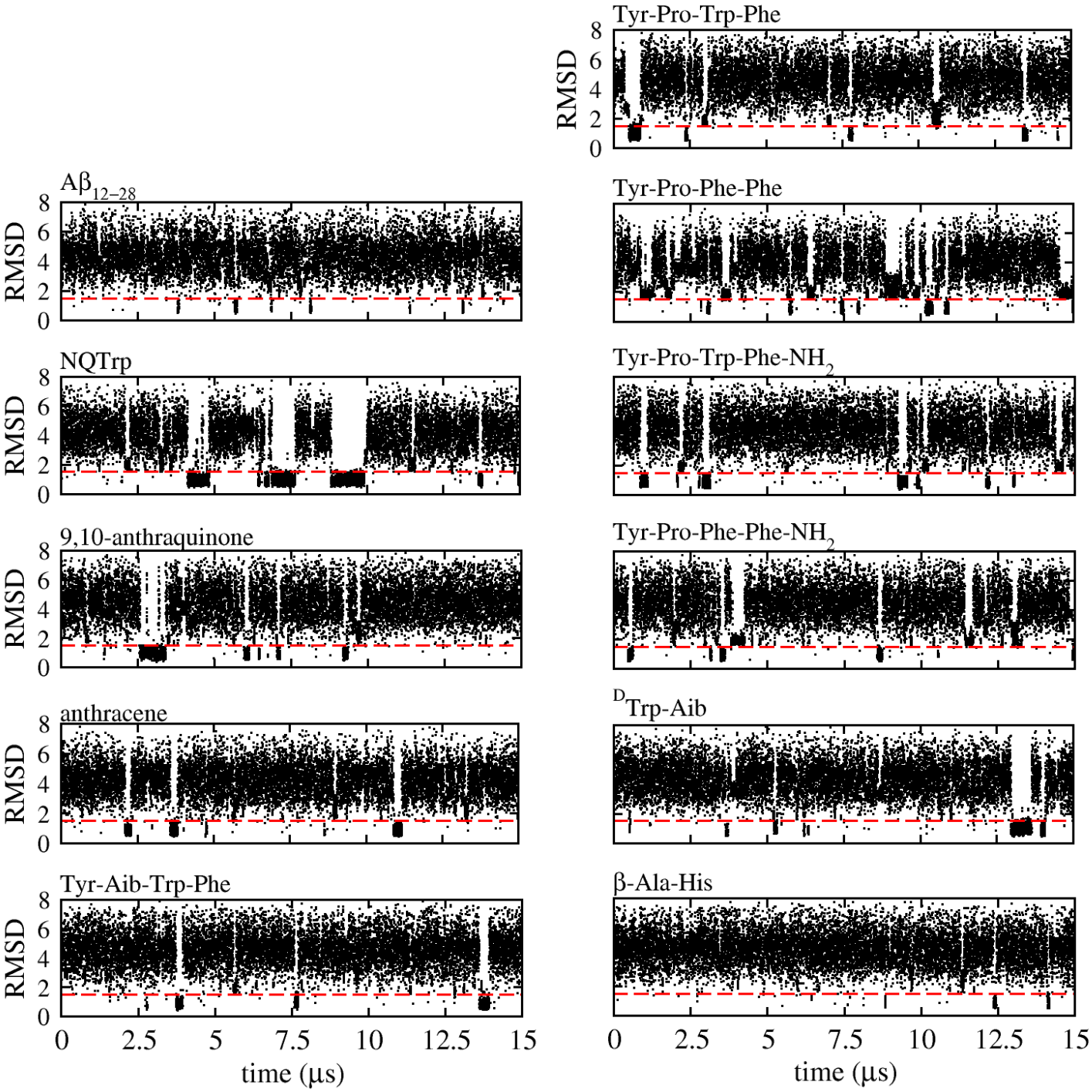

Figure S13. Time series of Cα RMSD from the representative node of the most populated cluster in simulations of Aβ_{12-28} in the presence of NQTrp (loop conformer). The Cα atoms of residues 14-24 were used to calculate the RMSD. The red dashed line at 1.5 Å is only a guide to the eye.

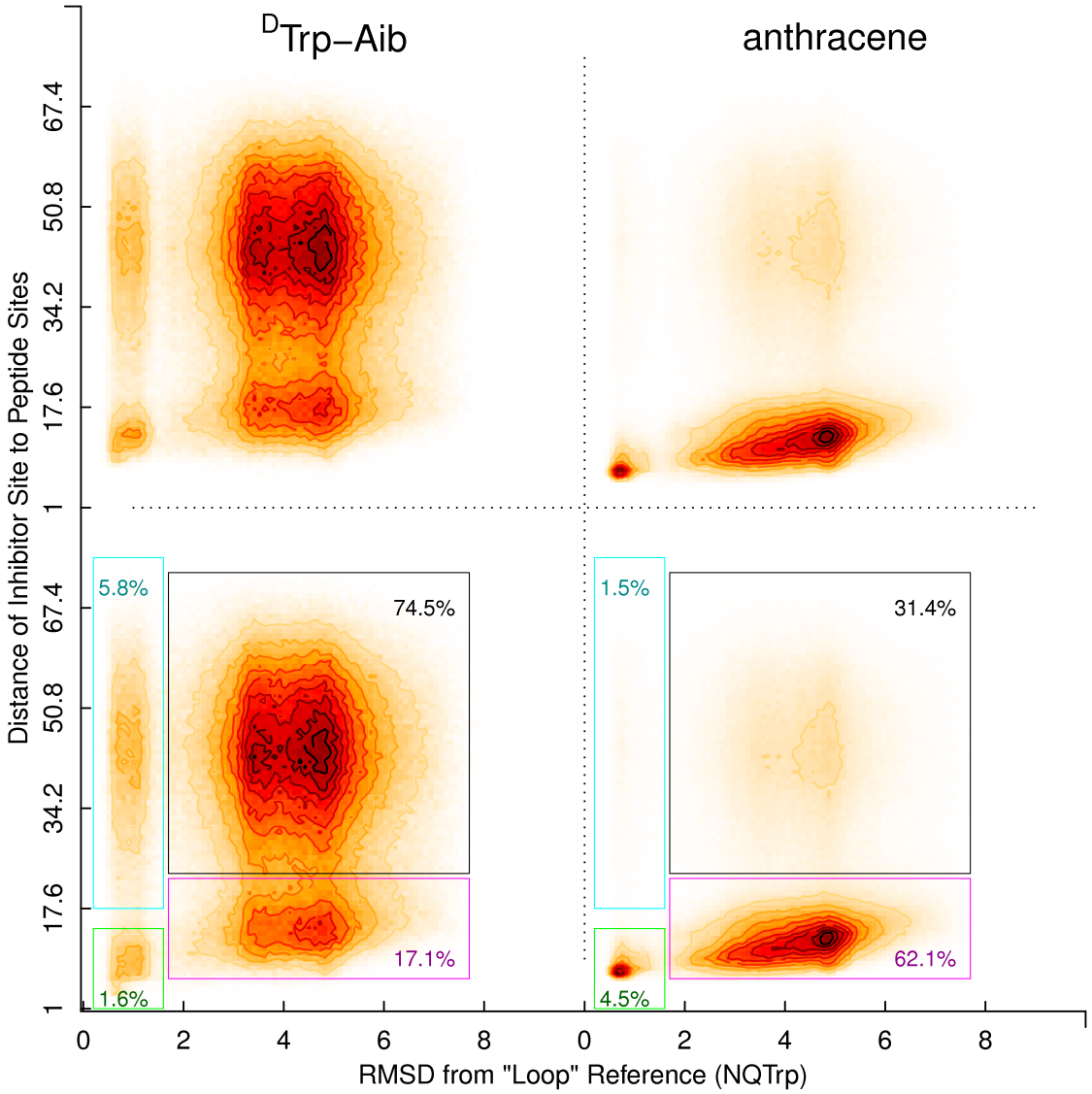

Figure S14. Two-dimensional histograms of the RMSD over Cα atoms of residues 14-24 to a reference structure and site-site distances between inhibitor and peptide. The chosen reference structure was the representative node of the most populated cluster for the system in which the loop structure was most strongly populated, i.e., A$\beta_{12\text{-}28}$ in the presence of NQTrp. Here, two different inhibitors are analyzed: ^{D}Trp-Aib (left column), and anthracene (right column). The sites on the peptide were the side chain oxygen atoms of Asp23 and Gln15. For ^{D}Trp-Aib, site-site correlation functions were computed to the polar indole nitrogen (lower left) or to the N-terminal, charged nitrogen (upper left). For anthracene, the sites considered were the four terminal carbons (lower right), and the two central carbons (upper right). In all cases, the distance axis can be used to distinguish bound from unbound states, and the RMSD axis can be used to distringuish loop-like from other conformations. Due to the good separation between states, the bottom row contains approximate sums of probabilities in the indicated, rectangular regions. These data indicate that anthracene

stabilizes the loop largely by direct interaction, whereas the impact of ^{D}Trp-Aib can also be indirect. The latter could be the result of both allosteric and memory effects.